Zwitterionic Iridium Complexes: Synthesis, Luminescent Properties, and Their Application in Cell Imaging

Weili Jiang,[†] Yuan Gao,[‡] Yun Sun,[‡] Fei Ding,[†] Yan Xu,[†] Zuqiang Bian,*[,†] Fuyou Li,[‡] Jiang Bian,*[,†] and Chunhui Huang[†,‡]

[†]*Beijing National Laboratory for Molecular Sciences, State Key Laboratory of Rare Earth Materials Chemistry and Applications, College of Chemistry and Molecular Engineering, Peking University, Beijing, 100871, China,* and [‡]*Department of Chemistry & Advanced Materials Laboratory, Fudan University, Shanghai, 200433, China*

A series of phosphorescent zwitterionic iridium(III) complexes, with 4-carboxy-2, 2′-bipyridine-4′-carboxylate (Hdcbpy) as ancillary ligand, Ir(C^N)$_2$(Hdcbpy) (C^N = 1-phenylpyrazole (ppz), 1-phenyl-pyridine (ppy), 2-(4′,6′-difluoro-phenyl)pyridine (dfppy), 1-phenyl-isoquinoline (piq), dibenzo[*f,h*]quinoxaline (dbq)), were prepared and characterized. Their photophysical properties were studied, and intense luminescence emissions were observed based on metal-to-ligand-charge-transfer (^{3}MLCT), ligand-to-ligand charge-transfer (^{3}LLCT), ligand-centered transitions (^{3}LC, i.e., $^3\pi \rightarrow \pi^*$), or intraligand-charge-transfer (^{3}ILCT) excited states, which were confirmed by theoretical calculations. The quantum yield of Ir(dfppy)$_2$(Hdcbpy) is as high as 0.106 in aqueous solution. With Hdcbpy as a hydrophilic part, their amphiphilic structures as further confirmed by X-ray single crystal data endow them with different solubilities in phosphate buffer solution (PBS, pH 7.0). The compounds were successfully applied as luminescent dyes for cell imaging in aqueous solution. Their different stain ability in cell imaging was fairly well supported by the experimental data based on the measurement of oil/water partition coefficients and encapsulation/release with liposomes.

Introduction

Life science and pathology require that increasingly more chemical techniques be developed to resolve problems that cannot be solved by conventional medical methods. One of the most convenient and effective ways to study the details in a cell is by fluorescent bioimaging with fluorescent dyes as labels because fluorescence bioimaging offers a unique approach for visualizing morphological details with subcellular resolution that cannot be resolved by ultrasound or magnetic resonance imaging.[1−3] Today, most of the fluorescent probes used are still organic fluorophores.[4] Organic fluorophores, however, have some limitations such as easy photobleaching, small Stokes shifts, and difficulty to filter the autofluorescence of certain organisms.[5] On the contrary, phosphorescent transition-metal complexes having metal-to-ligand-charge-transfer (^{3}MLCT) luminescence exhibit not only larger Stokes shifts but also much longer lifetimes as well as higher stability, making them better candidates as bioimaging probes. In this field, phosphorescent tetrahedral platinum(II) complexes have been well investigated, particularly owing to their good solubility in aqueous solution. Che et al.[6] and Lam et al.[7] respectively reported zwitterionic platinum(II) complexes with amphiphilic structures as imaging agents in aqueous solution while Williams et al.[8] opened up the microsecond domain in imaging in the nuclei with bright emissive platinum(II) complexes. As to the octahedral complexes, apart from that, Barton et al. explored cellular uptake of RuL$_2$dppz^{2+} (dppz = dipyridophenazine),[9] Coogan et al. reported the effects of sulfonated groups and hydrophobic carbon chains of rhenium(I) complexes in cellular uptake,[5]

*To whom correspondence should be addressed. E-mail: bianzq@pku.edu.cn (Z.B.), bj@pku.edu.cn (J.B.). Phone: (+86)10-6275-3544. Fax: (+86)10-6275-7156.

(1) Stephens, D. J.; Allan, V. J. *Science* **2003**, *300*, 82–86.
(2) Zhang, M.; Yu, M. X.; Li, F. Y.; Zhu, M. W.; Li, M. Y.; Gao, Y. H.; Li, L.; Liu, Z. Q.; Zhang, J. P.; Zhang, D. Q.; Yi, T.; Huang, C. H. *J. Am. Chem. Soc.* **2007**, *129*, 10322–10323.
(3) Yu, M. X.; Li, F. Y.; Chen, Z. G.; Hu, H.; Zhan, C.; Yang, H.; Huang, C. H. *Anal. Chem.* **2009**, *81*, 930–935.
(4) Haugland, R. P. Molecular Probes. In *A Guide to Fluorescent Probes and Labelling Technologies*, 10th ed.; Molecular Probes: Eugene, OR, 2005; www.probes.com and www.invitrogen.com.
(5) Amoroso, A. J.; Coogan, M. P.; Dunne, J. E.; Fernandez-Moreira, V.; Hess, J. B.; Hayes, A. J.; Lloyd, D.; Millet, C.; Pope, S. J. A.; Williams, C. *Chem. Commun.* **2007**, 3066–3068.

(6) Wu, P.; Wong, E. L. M.; Ma, D. L.; Tong, G. S. M.; Ng, K. M.; Che, C. M. *Chem.—Eur. J.* **2009**, *15*, 3652–3656.
(7) Koo, C. K.; Wong, K. L.; Man, C. W. Y.; Tam, H. L.; Tsao, S. W.; Cheah, K. W.; Lam, M. H. W. *Inorg. Chem.* **2009**, *48*, 7501–7503.
(8) Botchway, S. W.; Charnley, M.; Haycock, J. W.; Parker, A. W.; Rochester, D. L.; Weinstein, J. A.; Williams, J. A. G. *Proc. Natl. Acad. Sci. U.S.A.* **2008**, *105*, 16071–16076.
(9) Puckett, C. A.; Barton, J. K. *J. Am. Chem. Soc.* **2007**, *129*, 46–47.

Scheme 1. Synthetic Procedure of the Iridium Complexes

L1= ppz   L2 = ppy   L3 = dfppy   L4 = piq   L5 = dbq
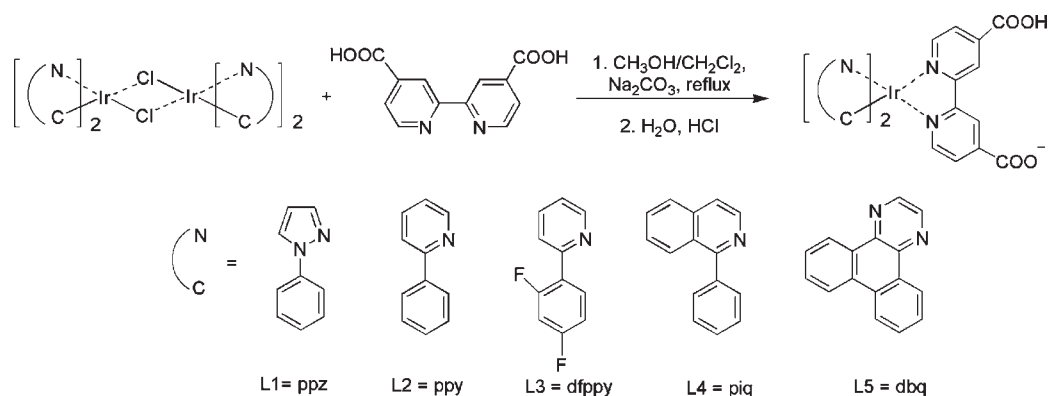
and Sheldrick et al. studied the cellular uptake of rhodium-(III) complexes.[10−12]

Compared with other transition-metal complexes, cyclo-metalated iridium(III) complexes have attracted great attention among chemists because of the strong spin−orbit coupling of the iridium ion (coupling constant, $\xi_{Ir} = 3909$ cm^{-1}),[13] high quantum yield in organic solvent, and tunable emission wave-lengths from blue to red.[14−18] To date, luminescent iridium(III) complexes have been applied in many fields such as organic light-emitting diodes (OLED),[19−23] chemical sensors,[24−27] and biological labeling reagents.[16,28−33] However, as the lumines-cent octahedral iridium(III) complexes are usually not soluble in aqueous solution, most of those used in the staining of organisms are cationic compounds with diamine ligands partly because of their ionic character. Thus, one of the challenges is how to improve the solubility of iridium(III) compounds in water. Lo et al. presented the first luminescent iridium(III) complexes for labeling biological substrates and have made a series of studies in this field.[28−34] Previously we successfully incubated HeLa cells with iridium(III) compounds in DMSO/PBS (pH 7.0) (1:49, v/v),[16] and this ratio was later reduced to 1:99 by Lo et al.[32] Another way to solve this problem is to adopt a charge-separated zwitterionic complex (a positive metal fragment and a negative charged ligand). Yet zwitterionic iridium(III) complexes are much less common[35] especially for those with luminescent character.[36]

The bipyridine ligand has been widely used in luminescent transition-metal complexes[37] while the derivative with a carbo-xyl substituent group has an acid/base equilibrium, which causes its complexes to be both water-soluble and oil-soluble.[38] By introducing the bipyridine ligand with carboxyl group, herein, we present a series of zwitterionic iridium(III) com-plexes, Ir(C$^\wedge$N)$_2$(Hdcbpy) (Hdcbpy = 4-carboxy-2, 2′-bipyri-dine-4′-carboxylate; C$^\wedge$N = 1-phenylpyrazole (ppz), 1-phenyl-pyridine (ppy), 2-(4′,6′-difluoro-phenyl)pyridine(dfppy), 1-phenyl-isoquinoline (piq) and dibenzo[*f,h*]quinoxaline(dbq), see Scheme 1). These iridium(III) complexes are amphiphilic and can be dissolved in PBS (pH 7.0). The color-tunable lumin-escence emission of these complexes was explored by varying the chemical structures of the cyclometalating ligands. Further-more, the interaction of KB cells with these complexes was investigated in detail, and the effect of amphiphilicity on the ability to permeate cell membranes was systematically studied.

Experimental Section

Materials and Instruments. All reagents and solvents were of analytical grade except those employed in photophysical

(10) Scharwitz, M. A.; Ott, I.; Geldmacher, Y.; Gust, R.; Sheldrick, W. S. *J. Organomet. Chem*. **2008**, *693*, 2299–2309.

(11) Bieda, R.; Ott, I.; Gust, R.; Sheldrick, W. S. *Eur. J. Inorg. Chem.* **2009**, 3821–3831.

(12) Harlos, M.; Ott, I.; Gust, R.; Alborzinia, H.; Wolfl, S.; Kromm, A.; Sheldrick, W. S. *J. Med. Chem.* **2008**, *51*, 3924–3933.

(13) Montalti, M. C., A.; Prodi, L.; Gandolfi, M. T. *Handbook of Photochemistry*; CRC Press: Boca Raton, FL, 2006.

(14) Lowry, M. S.; Bernhard, S. *Chem.—Eur. J.* **2006**, *12*, 7970–7977.

(15) Coughlin, F. J.; Westrol, M. S.; Oyler, K. D.; Byrne, N.; Kraml, C.; Zysman-Colman, E.; Lowry, M. S.; Bernhard, S. *Inorg. Chem.* **2008**, *47*, 2039–2048.

(16) Yu, M. X.; Zhao, Q.; Shi, L. X.; Li, F. Y.; Zhou, Z. G.; Yang, H.; Yia, T.; Huang, C. H. *Chem. Commun.* **2008**, 2115–2117.

(17) Zhao, Q.; Li, L.; Li, F. Y.; Yu, M. X.; Liu, Z. P.; Yi, T.; Huang, C. H. *Chem. Commun.* **2008**, 685–687.

(18) Huang, K. W.; Wu, H. Z.; Shi, M.; Li, F. Y.; Yi, T.; Huang, C. H. *Chem. Commun.* **2009**, 1243–1245.

(19) Baldo, M. A.; Lamansky, S.; Burrows, P. E.; Thompson, M. E.; Forrest, S. R. *Appl. Phys. Lett.* **1999**, *75*, 4–6.

(20) Adachi, C.; Baldo, M. A.; Forrest, S. R.; Lamansky, S.; Thompson, M. E.; Kwong, R. C. *Appl. Phys. Lett.* **2001**, *78*, 1622–1624.

(21) Liu, Z. W.; Guan, M.; Bian, Z. Q.; Nie, D. B.; Gong, Z. L.; Li, Z. B.; Huang, C. H. *Adv. Funct. Mater.* **2006**, *16*, 1441–1448.

(22) Liu, Z. W.; Bian, Z. Q.; Hao, F.; Nie, D. B.; Ding, F.; Chen, Z. Q.; Huang, C. H. *Org. Electron.* **2009**, *10*, 247–255.

(23) Liu, Z. W.; Bian, Z. Q.; Ming, L.; Ding, F.; Shen, H. Y.; Nie, D. B.; Huang, C. H. *Org. Electron.* **2008**, *9*, 171–182.

(24) Zhao, Q.; Cao, T. Y.; Li, F. Y.; Li, X. H.; Jing, H.; Yi, T.; Huang, C. H. *Organometallics* **2007**, *26*, 2077–2081.

(25) Zhao, Q.; Liu, S. J.; Li, F. Y.; Yi, T.; Huang, C. H. *Dalton Trans.* **2008**, 3836–3840.

(26) Chen, H. L.; Zhao, Q.; Wu, Y. B.; Li, F. Y.; Yang, H.; Yi, T.; Huang, C. H. *Inorg. Chem.* **2007**, *46*, 11075–11081.

(27) Liu, Z. W.; Bian, Z. Q.; Bian, J.; Li, Z. D.; Nie, D. B.; Huang, C. H. *Inorg. Chem.* **2008**, *47*, 8025–8030.

(28) Lo, K. K. W.; Ng, D. C. M.; Chung, C. K. *Organometallics* **2001**, *20*, 4999–5001.

(29) Lo, K. K. W.; Chung, C. K.; Lee, T. K. M.; Lui, L. H.; Tsang, K. H. K.; Zhu, N. Y. *Inorg. Chem.* **2003**, *42*, 6886–6897.

(30) Lo, K. K. W.; Chung, C. K.; Zhu, N. Y. *Chem.—Eur. J.* **2003**, *9*, 475–483.

(31) Lo, K. K. W.; Hui, W. K.; Chung, C. K.; Tsang, K. H. K.; Ng, D. C. M.; Zhu, N. Y.; Cheung, K. K. *Coord. Chem. Rev.* **2005**, *249*, 1434–1450.

(32) Lau, J. S. Y.; Lee, P. K.; Tsang, K. H. K.; Ng, C. H. C.; Lam, Y. W.; Cheng, S. H.; Lo, K. K. W. *Inorg. Chem.* **2009**, *48*, 708–718.

(33) Zhang, K. Y.; Lo, K. K. W. *Inorg. Chem.* **2009**, *48*, 6011–6025.

(34) Lo, K. K. W.; Chung, C. K.; Ng, D. C. M.; Zhu, N. Y. *New J. Chem.* **2002**, *26*, 81–88.

(35) Cipot, J.; McDonald, R.; Ferguson, M. J.; Schatte, G.; Stradiotto, M. *Organometallics* **2007**, *26*, 594–608.

(36) Byun, Y.; Lyu, Y. Y.; Das, R. R.; Kwon, O.; Lee, T. W.; Park, Y. J. *Appl. Phys. Lett.* **2007**, 91.

(37) Kaes, C.; Katz, A.; Hosseini, M. W. *Chem. Rev.* **2000**, *100*, 3553–3590.

(38) Waern, J. B.; Desmarets, C.; Chamoreau, L. M.; Amouri, H.; Barbieri, A.; Sabatini, C.; Ventura, B.; Barigelletti, F. *Inorg. Chem.* **2008**, *47*, 3340–3348.

experiments which were of spectroscopic grade. 1-Phenylpyrazole (ppz) and 1-phenyl-pyridine (ppy) were purchased from Alfa Aesar Chemical Co., and 2,2′-bipyridine-4,4′-dicarboxylic acid (H_2dcbpy) was purchased from Chemzam PharmTech Co. (China). All of them were directly used without further purification. 2-(4′,6′-Difluoro-phenyl)pyridine (dfppy),[39] dibenzo[f,h]-quinoxaline (dbq),[40] and 1-phenyl-isoquinoline (piq)[41] were prepared and purified according to previously published literatures. The phosphate buffer solution (PBS) used here is 50 mM potassium phosphate (pH 7.0). 1,2-Dimyristoyl-sn-glycero-3-phosphocholine (DMPC) and Cholesterol (Chol) were purchased from Sigma-Aldrich Chemical Co. KB cell line was provided by the Institute of Biochemistry and Cell Biology, SIBS, CAS (China).

The ^{1}H NMR spectra were recorded on an ARX-400 NMR spectrometer. The chemical shift data of each compound were reported in parts per million with tetramethylsilane as the internal reference. Elemental analyses (C, H, N) were performed on an Elementar Vario MICRO CUBE. High-resolution mass spectra were carried out on a Bruker Apex IV FTMS. The X-ray diffraction data were collected on a Rigaku MicroMax-007 CCD diffractometer using graphite-monochromated Mo/KR (λ = 0.71073 Å) radiation. Full crystallographic data are provided in CIF file format as Supporting Information and are available from the Cambridge Crystallographic Data Centre (CCDC-764064, 764065). The UV−vis absorption spectra were measured on a Shimadzu UV-3100 spectrometer. The photoluminescence (PL) spectra and lifetime data were obtained on an Edinburgh Analytical Instruments FLS920 spectrometer, and the spectra were corrected by the built-in program on the instrument. Luminescence quantum yields (Φ) in different solvents were measured at room temperature with an aerated aqueous solution of [Ru(bpy)$_3$]Cl$_2$ (Φ_r = 0.028)[42] as a standard. Confocal luminescence imaging was performed with an OLYMPUS IX81 laser scanning microscope and a 60X oil-immersion objective lens.

Synthesis of Iridium(III) Complexes. All of the complexes were synthesized by the same procedure. Cyclometalated iridium(III) dimers (C^N)$_2$Ir(μ-Cl)$_2$Ir(C^N)$_2$ were synthesized through the Nomoyama route, by refluxing IrCl$_3$·3H$_2$O with 2.2 equiv of the corresponding cyclometalating ligand (**L1-L5**) in 2-ethoxyethanol mixed with water (3:1) for 24 h. The suspension of 2,2′-bipyridine-4,4′-dicarboxylic acid (H$_2$dcbpy, 0.44 mmol) in CH$_3$OH (15 mL) was mixed with a solution of (C^N)$_2$Ir(μ-Cl)$_2$Ir(C^N)$_2$ (0.2 mmol) in CH$_2$Cl$_2$ (15 mL). Excessive Na$_2$CO$_3$ (1 mmol) was added to the reaction mixture which was then heated to reflux under stirring for 3 h. After having cooled to room temperature, the solvent was removed under reduced pressure, and deionized water (10 mL) was added to the residue. The pH of the solution was tuned to about 5 with dilute hydrochloric acid. The resulting precipitate was filtered as crude product which was then dissolved in a mixture of CH$_2$Cl$_2$ and CH$_3$OH (~3:1). After being dried with anhydrous sodium sulfate, the mixture was condensed and purified through a silica column with CH$_2$Cl$_2$/CH$_3$OH (1:1) for the elution.

Ir(ppz)$_2$(Hdcbpy) (1). Yield 91%. ^{1}H NMR (400 MHz, CDCl$_3$): δ 8.01 (2H, d, J = 1.8 Hz), 7.91 (2H, d, J = 5.6 Hz), 7.64 (2H, d, J = 5.6 Hz), 7.08 (2H, d, J = 8.0 Hz), 6.73 (2H, t, J = 7.2 Hz), 6.58 (2H, d, J = 2.0 Hz), 6.54 (2H, t, J = 7.6 Hz), 6.23 (2H, t, J = 2.4 Hz), 5.95 (2H, d, J = 7.2 Hz). Anal. Found for C$_{30}$H$_{21}$IrN$_6$O$_4$·H$_2$O: C, 49.04; H, 3.01; N, 11.39. Calcd: C,

48.71; H, 3.13; N, 11.36. HRMS (ESI$^+$, CH$_3$OH) calcd for C$_{30}$H$_{22}$IrN$_6$O$_4$, 723.1332 ([M+H]$^+$); found, 723.1331.

Ir(ppy)$_2$(Hdcbpy) (2). Yield 82%. ^{1}H NMR (400 MHz, CDCl$_3$): δ 8.08 (2H, d, J = 5.6 Hz), 7.98−8.03 (4H, m), 7.82 (2H, t, J = 7.6 Hz), 7.74 (2H, d, J = 7.2 Hz), 7.47 (2H, d, J = 5.2 Hz), 7.08 (2H, t, J = 7.6 Hz), 7.00 (2H, t, J = 6.4 Hz), 6.96 (2H, t, J = 6.8 Hz). Anal. Found for C$_{34}$H$_{23}$IrN$_4$O$_4$·2H$_2$O: C, 52.41; H, 3.48; N, 7.02. Calcd: C, 52.37; H, 3.49; N, 7.18. HRMS (ESI$^+$, CH$_3$OH) calcd for C$_{34}$H$_{24}$IrN$_4$O$_4$, 745.1427 ([M+H]$^+$); found, 745.1431.

Ir(dfppy)$_2$(Hdcbpy) (3). Yield 83%. ^{1}H NMR (400 MHz, CDCl$_3$): δ 9.13 (2H, s), 8.28 (2H, d, J = 8.0 Hz), 8.02 (2H, t, J = 8.0 Hz), 7.90−7.98 (4H, m), 7.72 (2H, d, J = 8.0 Hz), 7.22 (2H, t, J = 7.2 Hz), 6.95−7.01 (2H, ddd, J = 2.0 Hz, J = 9.6 Hz, J = 12.4 Hz), 5.59−5.62 (2H, dd, J = 2.3 Hz, J = 8.4 Hz). Anal. Found for C$_{34}$H$_{19}$F$_4$IrN$_4$O$_4$·2H$_2$O: C, 48.10; H, 2.72; N, 6.57. Calcd: C, 47.94; H, 2.72; N, 6.58. HRMS (ESI$^+$, CH$_3$OH) calcd for C$_{34}$H$_{20}$F$_4$IrN$_4$O$_4$, 817.1050 ([M+H]$^+$); found, 817.1023.

Ir(piq)$_2$(Hdcbpy) (4). Yield 76%. ^{1}H NMR (400 MHz, CDCl$_3$): δ 9.37 (2H, s), 8.96−8.98 (2H, q, J = 4.0 Hz, J = 6.4 Hz), 8.31 (2H, d, J = 8.0 Hz), 7.97 (2H, d, J = 5.2 Hz), 7.88−7.94 (4H, m), 7.80−7.84 (4H, q, J = 3.2 Hz, J = 10.0 Hz), 7.33 (4H, s), 7.16 (2H, t, J = 7.2 Hz), 6.94 (2H, t, J = 7.6 Hz), 6.30 (2H, d, J = 6.8 Hz). Anal. Found for C$_{42}$H$_{27}$IrN$_6$O$_4$·2H$_2$O: C, 56.80; H, 3.49; N, 6.27. Calcd: C, 57.33; H, 3.55; N, 6.37. HRMS (ESI$^+$, CH$_3$OH) calcd for C$_{42}$H$_{28}$IrN$_6$O$_4$, 845.1740 ([M+H]$^+$); found, 845.1722.

Ir(dbq)$_2$(Hdcbpy) (5). Yield 31%. ^{1}H NMR (400 MHz, CDCl$_3$): δ 9.23 (2H, d, J = 8.0 Hz), 9.18 (2H, s), 8.72 (2H, s), 8.63 (2H, d, J = 8.0 Hz), 8.19 (2H, d, J = 8.0 Hz), 8.02 (2H, s), 7.82−7.90 (8H, m), 7.32 (2H, t, J = 7.6 Hz), 6.43 (2H, d, J = 7.2 Hz). Anal. Found for C$_{44}$H$_{25}$IrN$_6$O$_4$·4H$_2$O: C, 54.33; H, 3.24; N, 8.60. Calcd: C, 54.71; H, 3.44; N, 8.70. HRMS (ESI$^+$, CH$_3$OH) calcd for C$_{44}$H$_{26}$IrN$_6$O$_4$, 895.1645 ([M+H]$^+$); found, 895.1643.

Theoretical Calculations. Both the singlet restrained and triplet unrestrained geometries were optimized by using the DFT method with the B3LYP hybrid functional. The LANL2DZ relativistic effective core potential was applied to describe the core electrons of iridium atoms, and full-electron calculations were carried out for the other atoms with 6-31G* basis set. The excited states of the complexes were calculated by using time-dependent density functional theory (TD-DFT) at the optimized triplet geometries. All of the calculations were carried out with the Gaussian 03 program.[43]

Solubility. The solubility of each complex in PBS was measured according to a published method.[44] Certain amount iridium complex (about 20 mg for complexes **1−2** or 5 mg for **3−5**) was suspended in about 5 mL of PBS. The suspension was sonicated for 30 min and then stirred for 20 h at room temperature (290 K). The resulting mixture was filtered through a 0.2 μm

(39) You, Y.; Kim, S. H.; Jung, H. K.; Park, S. Y. *Macromolecules* **2006**, *39*, 349–356.

(40) Duan, J. P.; Sun, P. P.; Cheng, C. H. *Adv. Mater.* **2003**, *15*, 224–228.

(41) Tsuboyama, A.; Iwakaki, H.; Furugori, M.; Mukaide, T.; Kamatani, J.; Igawa, S.; Moriyama, T.; Miura, S.; Takiguchi, T.; Okada, S.; Hoshino, M.; Ueno, K. *J. Am. Chem. Soc.* **2003**, *125*, 12971–12979.

(42) Nakamaru, K. *Bull. Chem. Soc. Jpn.* **1982**, *55*, 2697–2705.

(43) Frisch M. J., T. G. W., Schlegel H. B., Scuseria G. E., Robb M. A., Cheeseman J. R., Montgomery J. A., Jr.,Vreven T., Kudin K. N., Burant J. C., Millam J. M., Iyengar S. S.,Tomasi J., Barone V., Mennucci B.,Cossi M.,Scalmani G., Rega N., Petersson G. A., Nakatsuji H., Hada M.,Ehara M., Toyota K., Fukuda R., Hasegawa J.,Ishida M., Nakajima T., Honda Y.,Kitao O., Nakai H., Klene M., Li X., KnoxJ. E., Hratchian H. P., Cross J. B., Bakken V.,Adamo C., Jaramillo J., Gomperts R., Stratmann R. E., Yazyev O., Austin, A. J., Cammi R., Pomelli C., Ochterski J. W., Ayala P. Y., Morokuma K., Voth G. A., Salvador P., Dannenberg J. J.,Zakrzewski V. G., Dapprich S., Daniels A. D., Strain M. C., Farkas O., Malick D. K., Rabuck A. D., Raghavachari K., Foresman J. B., Ortiz J. V., Cui Q., Baboul A. G., Clifford S., Cioslowski J., StefanovB. B., Liu G., Liashenko A., Piskorz P., Komaromi I., Martin R. L., Fox D. J., Keith T., Al-Laham M. A., Peng C. Y., Nanayakkara A., Challacombe M., Gill P. M. W., Johnson B., Chen W.,Wong M. W., Gonzalez C., Pople J. A. *Gaussian 03*, Revision D.02; Gaussian, Inc.: Wallingford, CT, 2004.

(44) Park, J. W.; Ahn, J. H.; Lee, C. *J. Photochem. Photobiol. A: Chem.* **1995**, *86*, 89–95.
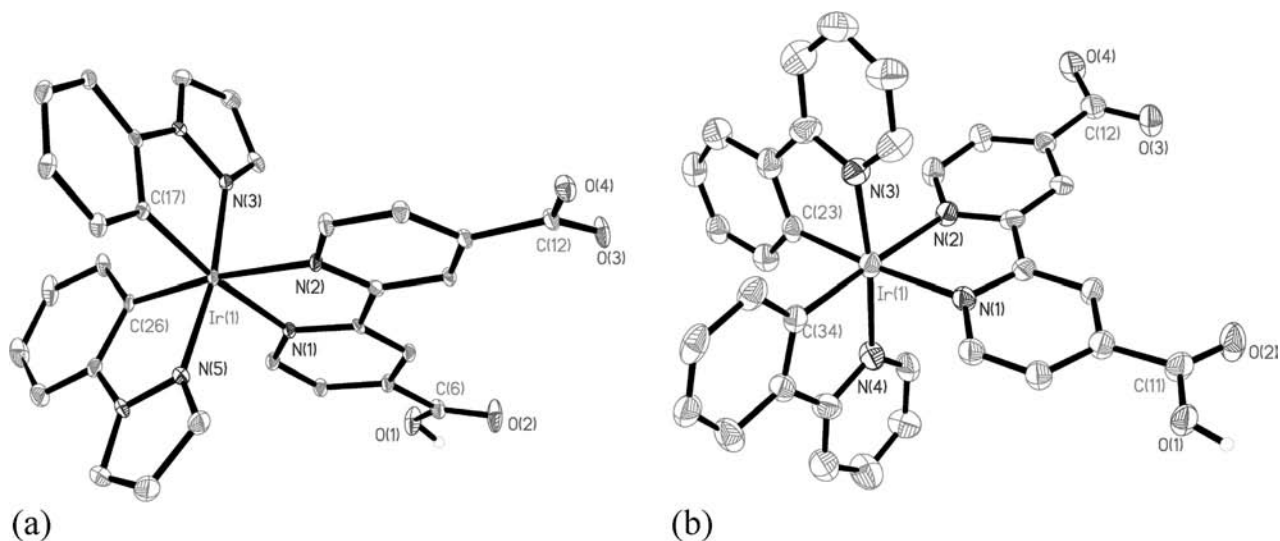
Figure 1. X-ray crystal structure of **1** (a) and **2** (b) with thermal ellipsoids drawn at the 30% probability level. H atoms (except the one on the carboxyl group) and solvent molecules were omitted for clarity.

Millipore filter before diluted with PBS. The concentration of the complex in the dilute solution was determined by spectrophotometry.

Amphiphilicity. The octanol−water partition coefficient, $P_{o/w}$ (or log $P_{o/w}$), is a measure of material amphiphilicity. It represents the relative solubility of a material in oil and water. The octanol−water partition coefficient experiment was performed on an HY-4 Oscillator by a classical method in accordance with the literature.[45] Equal amounts of *n*-octanol and PBS were thoroughly mixed by an oscillator for 24 h. The mixture was then left to separate for another 24 h to finally yield water and octanol phase, each saturated with the other. Each complex was carefully dissolved in PBS (concentration corresponded to c_o) and PBS saturated with octanol to form a 20 μM solution. Then the latter was mixed with equal amounts of octanol (saturated with water) and shaken again as described above. After separation, the final concentrations of compounds in water corresponded to c_w. Both c_o and c_w were measured by spectrophotometry at $\lambda = 310$ nm, and the partition coefficient ($P_{o/w}$) for each complex was calculated by the following equation:

$$P_{o/w} = (c_o - c_w)/c_w$$

Encapsulation into Liposomes and Release. A 3.5 mg portion of DMPC and 1.65 mg of Chol (55:45, mol/mol) were dissolved in 10 mL of chloroform. A 3.5 mg portion of iridium complex was added to the mixture which was then sonicated for 30 min to facilitate the dissolving process. A lipid thin film was obtained by evaporating the solvent under reduced pressure and suspended in 15 mL of PBS by sonication to give liposomes encapsulated with complex. Unencapsulated complex was removed by dialyzing against 1000 mL of PBS through a cellulose dialysis membrane. Then the dialysis membrane was placed into 20 mL of PBS for 12 h to achieve an equilibrium. The concentration (c_1) of the solution outside the dialysis membrane was determined by spectrophotometry. Subsequently, the membrane was cut off, and 1 mL of 1% SDS (sodium dodecyl sulfate)-PBS solution was added to destroy the liposomes. After a short sonication, the concentration (c_2) of the complex was determined by spectrophotometry. The encapsulation efficiency of iridium(III) complex into liposomes was calculated as follows: encapsulation efficiency (%) = $[c_2 V_2/3.5 \text{ mg}] \times 100$,

$V_2 = 36$ mL. The release of the complex from liposomes was calculated by the following equation: release (%) = $[c_1 V_1/c_2 V_2] \times 100$, $V_1 = 35$ mL.

Cell Imaging. KB cells were grown in MEM (Modified Eagle's Medium) supplemented with 10% FBS (Fetal Bovine Serum) and 5% CO_2 at 37 °C. Cells (5×10^8/ L) were plated on 14 mm glass coverslips and allowed to adhere for 24 h. Fixed cells were those fixed by 4% paraformaldehyde for 1 h, and then washed with PBS three times. Each complex was applied in both living cells and fixed cells. First, the iridium(III) complex was dissolved in PBS to yield 10 μM and 20 μM solutions. Then both kinds of KB cells were incubated with each of the complex solutions (2 mL) for 0.5−2 h before washing with PBS. A semiconductor laser was used for excitation of the KB cells incubated with complexes **1**−**5** at 405 nm. Emission was collected at 530−630, 590−690, 490−590, 550−650, and 550−650 nm for KB cells incubated with complexes **1**−**5**, respectively.

Results and Discussion

Synthesis and Characterization. Scheme 1 shows the general synthesis route of the five iridium complexes **1**−**5**. The cyclometalated iridium(III) dimers were stirred with H_2dcbpy in a mixture of CH_3OH and CH_2Cl_2 (1:1) in the presence of excessive Na_2CO_3 under refluxing for 3 h. The preliminary iridium(III) product was acidified with dilute hydrochloric acid to pH 4−5. If the pH dropped below 3, the product would assume an acid form $(C^\wedge N)_2$Ir-$(H_2$dcbpy). The final electron-neutral product could be dissolved in water of pH 7.0. All the products were characterized through ^{1}H NMR, high-resolution mass spectrometry, and elemental analysis.

X-ray Crystal Structures of Complexes 1 and 2. The single crystals of **1** and **2** were obtained by slowly evaporating solvent from CH_2Cl_2/CH_3OH solution. X-ray crystallographic structures are shown in Figure 1, and crystallographic data are summarized in Table 1. Selected bond lengths are listed in Tables 2 and 3. As we expected, the two nitrogen atoms on Hdcbpy coordinate well with the centered iridium(III) ion because of the strong affinity of Ir for N, while two carboxyl groups are unfolded freely. In the octahedral geometry of the Ir center, N atoms from $C^\wedge N$ ligands adopt a trans-configuration, which is

(45) Sansgter, J. *Octanol-Water Partition Coefficients: Fundamentals and Physical Chemistry*; Wiley: Chichester, 1997.

Table 1. Crystal Data and Structure Refinement for **1** and **2**

	1	**2**
empirical formula	$C_{30}H_{21}IrN_6O_4$	$C_{34}H_{23}IrN_4O_4$
crystal system	monoclinic	monoclinic
space group	$P12_1/c1$	$P2(1)/n$
a (Å)	8.7068(13)	9.2108(18)
b (Å)	35.482(5)	14.495(3)
c (Å)	9.8564(15)	21.887(4)
α (deg)	90	90
β (deg)	91.918(3)	92.52(3)
γ (deg)	90	90
V (Å^3)	3043.3(8)	2919.3(10)
Z	4	4
ρ (calcd) (g·cm^{-3})	1.715	1.765
$F(000)$	1552	1528
θ range (deg)	2.15−27.88	1.69−27.14
GOF on F^2	1.050	1.190
final R indices	R1 = 0.0384,	R1 = 0.0700,
$[I > 2\sigma(I)]$	wR2 = 0.0898	wR2 = 0.1567
R indices	R1 = 0.0477,	R1 = 0.0814,
(all data)	wR2 = 0.0948	wR2 = 0.1634

Table 2. Selected Bond Lengths (Å) of **1**

Ir(1)−N(1)	2.116(4)	O(1)−H(1)	0.8400
Ir(1)−N(2)	2.133(3)	O(1)−C(6)	1.307(5)
Ir(1)−N(3)	2.022(4)	O(2)−C(6)	1.191(6)
Ir(1)−N(5)	2.023(4)	O(3)−C(12)	1.249(6)
Ir(1)−C(17)	2.037(5)	O(4)−C(12)	1.243(5)
Ir(1)−C(26)	2.012(4)		

Table 3. Selected Bond Lengths (Å) of **2**

Ir(1)−N(1)	2.115(7)	O(1)−H(1)	0.8400
Ir(1)−N(2)	2.134(7)	O(1)−C(11)	1.307(10)
Ir(1)−N(3)	2.023(9)	O(2)−C(11)	1.205(11)
Ir(1)−N(4)	2.056(8)	O(3)−C(12)	1.250(12)
Ir(1)−C(23)	2.018(9)	O(4)−C(12)	1.251(11)
Ir(1)−C(34)	2.019(8)		

common in many Ir(C^N)$_2$(LX) complexes.[38,46−48] At the given pH value, the hydrogen atom on one carboxyl is lost to meet the need for electroneutrality of the molecule. Such a structure makes the compounds soluble in PBS (pH 7.0). The bond lengths between Ir and N of Hdcbpy for both complexes are longer than those between Ir and N or C on cyclometalating ligands because of the trans-effect of the C donor in ppz (bonds trans to C atoms are longer than those trans to N atoms because of the σ donation of the carbons).[38,47,48] On the −COO$^-$ group, the distances between two O and C are very close, that is, the bond lengths are averaged; while for the −COOH group, the bond length between O on the −OH group and C is obviously longer than the C=O length showing the existence of the difference between single and double bond.

Photophysical Properties. The photophysical properties of complexes **1−5** in CH$_2$Cl$_2$, EtOH, and PBS were researched, and the data are summarized in Table 4. Figure 2 shows the UV−vis absorption spectra recorded in PBS at room temperature. In the high-energy region of 240−320 nm, all these compounds exhibit intense absorption bands with extinction coefficient $\varepsilon > 10\,000$ M^{-1} cm^{-1}, which are assigned to spin-allowed ligand-centered

transitions ^{1}LC ($^1\pi \to \pi*$) localizing on Hdcbpy and C^N ligands. The weak absorptions (2 000 $< \varepsilon <$ 10 000 M^{-1} cm^{-1}) at 320−410 nm are attributed to spin-allowed singlet-to-singlet metal-to-ligand charge-transfer (^{1}MLCT) and ligand-to-ligand charge-transfer (^{1}LLCT), which are common in iridium(III) compounds.[46,49−51] Weaker absorptions above 410 nm can be explained by spin-forbidden ^{3}LC transitions accompanied by some portion of ^{3}LLCT and ^{3}MLCT,[46,51−54] which was also confirmed by subsequent DFT calculations.

TD-DFT analysis was carried out to explore the nature of the excited states in the complexes. The optimized structures of compounds **1** and **2** are in good agreement with the crystallographic data (Supporting Information, Tables S1 and S2), which confirms that our computational model is suitable for the system despite the absence of the crystal structures for the other compounds. The molecular orbitals involved in the triplet electron transitions for compounds **1−5** are shown in Table 5, while the calculated wavelengths and designations are listed in Table 6. For all the compounds, the highest occupied molecular orbital (HOMO) is located mainly on the iridium(III) center and the phenyl groups of C^N ligands, while the lowest unoccupied molecular orbital (LUMO) lies primarily on the N^N ligands (Hdcbpy), which is in accord with previous calculations.[46,55−57] However, the electron transition does not originate from pure HOMO to LUMO, but from HOMO or HOMO-1 or HOMO-3 to LUMO or some orbitals above because of the selection rule of the spectrum. This is caused by the electron-withdrawing −COOH and −COO$^-$ groups on the bpy ligand which make the ligand a better acceptor and thus sufficiently stabilizes the LUMO, leading to a decrease in the energy gap.[58,59] By frontier orbital analysis we can clearly identify the nature of the excited states of the compounds, which mainly consists of a mixture of ^{3}MLCT [dπ(Ir) $\to \pi*_{N\wedge N}$], ^{3}LLCT [$\pi_{C\wedge N} \to \pi*_{\wedge N}$], and ^{3}LC [$\pi_{C\wedge N} \to \pi*_{C\wedge N}$], as a result of the close proximity of these states and the strong spin−orbit coupling effect.[28,46,50,60] As to complexes **4** and **5**, clear intraligand-charge-transfer (^{3}ILCT) is also observed

(46) Zhao, Q.; Liu, S. J.; Shi, M.; Wang, C. M.; Yu, M. X.; Li, L.; Li, F. Y.; Yi, T.; Huang, C. H. *Inorg. Chem.* **2006**, *45*, 6152−6160.

(47) Song, Y. H.; Yeh, S. J.; Chen, C. T.; Chi, Y.; Liu, C. S.; Yu, J. K.; Hu, Y. H.; Chou, P. T.; Peng, S. M.; Lee, G. H. *Adv. Funct. Mater.* **2004**, *14*, 1221−1226.
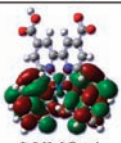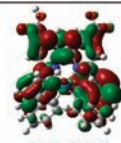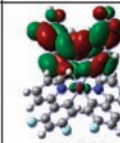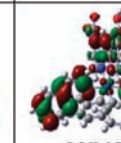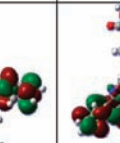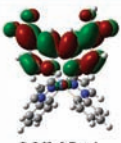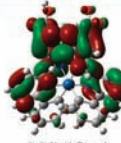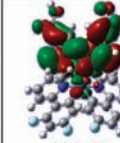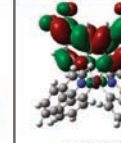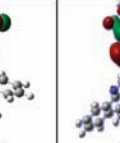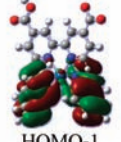
(48) Orselli, E.; Kottas, G. S.; Konradsson, A. E.; Coppo, P.; Frohlich, R.; De Cola, L.; van Dijken, A.; Buchel, M.; Borner, H. *Inorg. Chem.* **2007**, *46*, 11082−11093.

(49) Yeh, Y. S.; Cheng, Y. M.; Chou, P. T.; Lee, G. H.; Yang, C. H.; Chi, Y.; Shu, C. F.; Wang, C. H. *ChemPhysChem* **2006**, *7*, 2294−2297.

(50) Neve, F.; La Deda, M.; Crispini, A.; Bellusci, A.; Puntoriero, F.; Campagna, S. *Organometallics* **2004**, *23*, 5856−5863.

(51) Zhao, Q.; Jiang, C. Y.; Shi, M.; Li, F. Y.; Yi, T.; Cao, Y.; Huang, C. H. *Organometallics* **2006**, *25*, 3631−3638.

(52) Lamansky, S.; Djurovich, P.; Murphy, D.; Abdel-Razzaq, F.; Lee, H. E.; Adachi, C.; Burrows, P. E.; Forrest, S. R.; Thompson, M. E. *J. Am. Chem. Soc.* **2001**, *123*, 4304−4312.

(53) Sajoto, T.; Djurovich, P. I.; Tamayo, A.; Yousufuddin, M.; Bau, R.; Thompson, M. E.; Holmes, R. J.; Forrest, S. R. *Inorg. Chem.* **2005**, *44*, 7992−8003.

(54) Lamansky, S.; Djurovich, P.; Murphy, D.; Abdel-Razzaq, F.; Kwong, R.; Tsyba, I.; Bortz, M.; Mui, B.; Bau, R.; Thompson, M. E. *Inorg. Chem.* **2001**, *40*, 1704−1711.
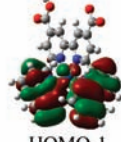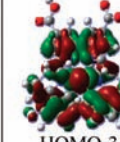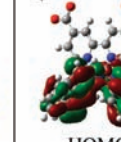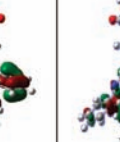
(55) Zhao, Q.; Li, F. Y.; Liu, S. J.; Yu, M. X.; Liu, Z. Q.; Yi, T.; Huang, C. H. *Inorg. Chem.* **2008**, *47*, 9256−9264.

(56) Stagni, S.; Colella, S.; Palazzi, A.; Valenti, G.; Zacchini, S.; Paolucci, F.; Marcaccio, M.; Albuquerque, R. O.; De Cola, L. *Inorg. Chem.* **2008**, *47*, 10509−10521.

(57) Lowry, M. S.; Goldsmith, J. I.; Slinker, J. D.; Rohl, R.; Pascal, R. A.; Malliaras, G. G.; Bernhard, S. *Chem. Mater.* **2005**, *17*, 5712−5719.

(58) Cherry, W. R.; Henderson, L. J. *Inorg. Chem.* **1984**, *23*, 983−986.

(59) Lumpkin, R. S.; Kober, E. M.; Worl, L. A.; Murtaza, Z.; Meyer, T. J. *J. Phys. Chem.* **1990**, *94*, 239−243.

(60) Colombo, M. G.; Hauser, A.; Gudel, H. U. *Inorg. Chem.* **1993**, *32*, 3088−3092.

Table 4. Photophysical Data of **1**−**5** in PBS, CH_2Cl_2, and EtOH[a] at Room Temperature and 77 K

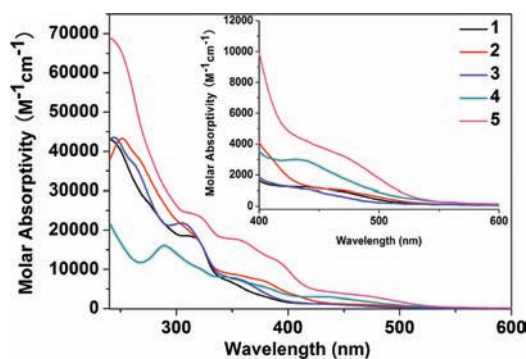|		absorption	emission (r.t.)			emission (77 K)	
	solvent	λ, nm (ε, 10^3 M^{-1} cm^{-1})	λ_{max}, nm	Φ^b	τ^b, ns	λ_{max}, nm	τ, μs
1	PBS	318(18.0), 352(6.4) sh, 443(1.2)	635	0.004	26		
	CH_2Cl_2	315(16.0), 361(5.6) sh	593	0.164(0.176)	318(387)		
	EtOH	314(15.9), 355(6.2) sh	574	0.114		541	3.7
2	PBS	251(43.0), 318(18.2) sh, 380(6.9)	651	0.004	17		
	CH_2Cl_2	253(21.7), 307(14.4), 370(5.7)	617	0.159(0.172)	277(302)		
	EtOH	264(37.8), 371(5.9)	592	0.083		542	4.1
3	PBS	244(43.5), 264(36.0) sh, 304(21.8), 357(7.2)	580	0.106	167		
	CH_2Cl_2	249(42.1), 264(38.5) sh, 313(21.2), 366(6.9)	543	0.351(0.393)	751(822)		
	EtOH	246(40.6), 307(21.4), 363(6.5) sh	519	0.361		502	5.2
4	PBS	289(16.1), 354(7.9), 380(5.3) sh, 436(3.0)	594(sh), 633	0.015	291		
	CH_2Cl_2	292(27.5), 356(12.1), 381(8.3) sh, 440(4.5)	594, 630	0.035(0.041)	491(679)		
	EtOH	288(36.7), 353(12.6), 382(8.0) sh, 441(4.8)	593, 630	0.030		580	4.3
5	PBS	319(23.7), 357(17.4), 391(12.0) sh, 461(3.5)	594	0.036	336		
	CH_2Cl_2	249(60.7), 319(19.6), 357(15.1) sh, 390(10.2) sh	572	0.190(0.212)	853(1173)		
	EtOH	250(68.2), 316(19.4), 354(16.6), 387(10.4) sh	600	0.053		529	6.5

[a] The concentrations of the complexes in each solvent were 10 μM. To address the solubility problem in CH_2Cl_2 or EtOH, the complexes were dissolved in a mixture of CH_2Cl_2 and MeOH (∼3:1) to a concentration of 1 mM and then diluted with CH_2Cl_2 or EtOH. [b] The values in parentheses are quantum yields or lifetimes measured in CH_2Cl_2 saturated with Ar gas.

Table 5. HOMO and LUMO Distributions for **1**−**5**

(from phenyl to isoquinolin or to benzo[*f*]quinoxaline group) because of the complicated cyclometalating ligands (piq and dbq).

Normalized luminescence spectra of complexes **1**−**5** in PBS are shown in Figure 3, and the corresponding photophysical data for different solvents are listed in Table 4. The luminescent emission color of the materials can be tuned from yellow to red by changing their C^N ligands. The origin of the yellow color of complex **3** is due to the two electron-withdrawing F atoms on the phenyl group of dfppy stabilizing the HOMO, resulting in an increase in the energy gap as well as a blue shift in the emission band. Additionally, broad and featureless emission bands for complexes **1**, **2**, **3**, and **5** with a large dependence on solvents indicate the CT character of the excited states,[46,50,61] whereas a

(61) Okada, S.; Okinaka, K.; Iwawaki, H.; Furugori, M.; Hashimoto, M.; Mukaide, T.; Kamatani, J.; Igawa, S.; Tsuboyama, A.; Takiguchi, T.; Ueno, K. *Dalton Trans.* **2005**, 1583–1590.
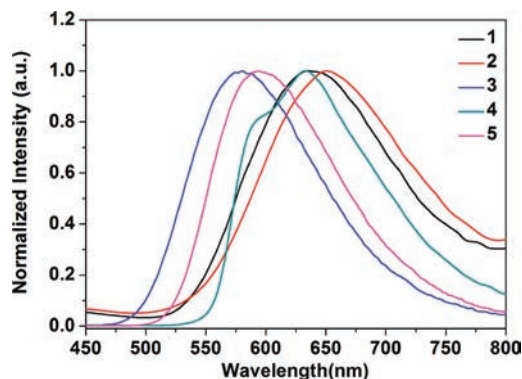

Figure 2. UV−vis absorption spectra of complexes **1**−**5** in PBS at room temperature.

vibronic-structured emission was detected for complex **4** accompanied by a much smaller dependence of luminescence on solvents. According to published

Figure 3. Normalized emission spectra of complexes **1−5** in PBS at room temperature.

works,[46,56,62,63] this is caused by the mixing of considerable percentages of ^{3}LC states with ^{3}MLCT states, as well as ^{3}ILCT [$\pi_{phenyl} \rightarrow \pi^*_{isoquinolin}$] possessing much higher LC character.[49] It is interesting to notice that the λ_{max} for complexes **1−3** in CH_2Cl_2 is longer than that in EtOH, while it is opposite for complex **5**. Generally, λ_{max} gets longer with the increase in polarity of solvents.[55] However, our complexes can ionize weakly in EtOH to produce a deprotonated form emitting at higher energy.[38] As to complex **5**, the much weaker ionization makes its λ_{max} longer in EtOH than in CH_2Cl_2. The luminescence in EtOH glass at 77 K for compounds **1−5** was also studied to give a more detailed picture of luminescent properties (Figure 4 and Table 4). As is to be expected, large blue shifts associated with some structure on the emission are observed for complexes **1−3** and **5**, confirming the charge transfer (CT) character of the compounds, which was widely studied in the last two decades[62,64,65] and explained as the fast solvent reorganization at room temperature which can stabilize the CT states before emission takes place, while the stabilization of CT states is hampered at 77 K.[50,55] Inversely, for complex **4**, only a much smaller shift was found owing to its strong LC character.

Finally, it is worth noting that the quantum yields of the complexes are relatively high (Table 4) in aerated water as well as in organic solvents, which has scarcely been reported before, especially for complex **3** whose quantum yield reaches 0.106 in water. When the solvent CH_2Cl_2 was saturated with Ar gas, the quantum yields and lifetimes all get a slight enhancement. The long lifetimes in solvents (submicrosecond scale at room temperature and microsecond scale at 77 K) confirm the phosphorescent character of the compounds' emissions.

Cell Imaging. The interaction of living cells with emissive iridium(III) complexes **1−5** was investigated in detail by laser scanning fluorescence microscopy. To compare the abilities of iridium(III) complexes **1−5** to stain cells,

KB cells were incubated with each complex in PBS in the same incubation time and concentration. Figure 5 shows the images of living KB cells incubated with complexes **1−5** at a concentration of 20 μM for 30 min. Interestingly, complexes **1−2** and **3−4** displayed no and weak intracellular luminescence, respectively; whereas complex **5** displayed very intense intracellular luminescence. These observations suggest that complexes **1−2** hardly entered the cells, and that complexes **3−4** did better, while complex **5** permeated very easily. The abilities of living cell membrane penetration for these iridium(III) compounds obey this order: **1 ≈ 2 < 3 ≈ 4 < 5**. Additionally, all KB cells were alive after 2 h incubation with these compounds, which reveals that these five iridium(III) complexes are minimally toxic.

Furthermore, we investigated the interaction of fixed cells with complexes **1−5**. KB cells fixed by 4% paraformaldehyde were loaded with these complexes. As shown in Figure 6, very weak and visible intracellular luminescence was observed for complex **2** and complexes **3−5**, respectively. Notably, no luminescence was detected for fixed KB cells incubated with complex **1** for 30 min. These findings indicate that the abilities of fixed cell membrane penetration for these iridium(III) compounds obey this order: **1 < 2 < 3−5**. It can be concluded from Figure 5 and Figure 6 that, the more hydrophilic complexes **1** and **2** have poor permeability; while the hydrophobic complexes **3−5** passed the membrane smoothly. The data in Table 7 are responsible for the different imaging abilities for complexes **1−5**.

From Figure 5 and Figure 6 we can also find that, after passing through the cell membrane, the compounds mainly stay in the cytoplasm for both living and fixed KB cells. This is further confirmed by Z-scan luminescence imaging of living and fixed KB cells incubated with these complexes (Figure 7 and Supporting Information). Figure 7 shows a three-dimensional luminescence image of living KB cells incubated with complex **5**. When further comparing with Figure 5, we can see that fixed KB cells facilitate penetration of these iridium(III) complexes into the cytoplasm. This may originate from the compromised membrane after being treated with paraformaldehyde, which could facilitate high penetrability of materials.[33]

Solubility and Solute Permeation Characteristics. Furthermore, the water-soluble properties, amphiphilicity, encapsulation, and release with liposomes of these complexes were carried out to investigate their different membrane permeation. The data were summarized in Table 7. When dissolved in PBS, the remaining −COOH on each complex may undergo ionization, as a two-step acid dissociation was observed for [Ru(DIP)$_2$-(H$_2$dcbpy)]$^{2+}$[38] and [Ru(bpy)$_2$(H$_2$dcbpy)]$^{2+}$.[66] However, the pK_a of the iridium(III) complexes is difficult to measure owing to their poor solubilities, which was also found in Waern at al.'s work.[38] As expected, because of the different cyclometalating ligands, the solubility of the complexes varies within a large range: complexes **1** and **2** have larger solubilities with a magnitude of millimolar, whereas the complex **5** with the largest cyclometalating ligand is just slight soluble in aqueous solution. For

(62) Juris, A.; Balzani, V.; Barigelletti, F.; Campagna, S.; Belser, P.; Vonzelewsky, A. *Coord. Chem. Rev.* **1988**, *84*, 85–277.

(63) Juris, A.; Campagna, S.; Bidd, I.; Lehn, J. M.; Ziessel, R. *Inorg. Chem.* **1988**, *27*, 4007–4011.

(64) Giordano, P. J.; Wrighton, M. S. *J. Am. Chem. Soc.* **1979**, *101*, 2888–2897.

(65) Barigelletti, F.; Belser, P.; Vonzelewsky, A.; Juris, A.; Balzani, V. *J. Phys. Chem.* **1985**, *89*, 3680–3684.

(66) Shimidzu, T.; Iyoda, T.; Izaki, K. *J. Phys. Chem.* **1985**, *89*, 642–645.

Table 6. Calculated Excited Triplet States and Character of the Transitions for the Complexes

	λ_{cal}, nm	E_{cal}, eV	excitation	nature of the excited states
1	609	2.04	HOMO-1 → LUMO+4 (0.61)	^{3}MLCT+^{3}LLCT+^{3}LC
			HOMO-1 → LUMO+1 (0.39)	
2	621	2.00	HOMO-1 → LUMO+6 (0.49)	^{3}MLCT+^{3}LLCT+^{3}LC
			HOMO-1 → LUMO+4 (0.32)	
3	504	2.46	HOMO-3 → LUMO (0.68)	^{3}MLCT+^{3}LLCT
4	614	2.01	HOMO-1 → LUMO+6 (0.51)	^{3}MLCT+^{3}LLCT+^{3}LC+^{3}ILCT
			HOMO-1 → LUMO+3 (0.40)	
5	582	2.13	HOMO → LUMO+8 (0.69)	^{3}MLCT+^{3}ILCT
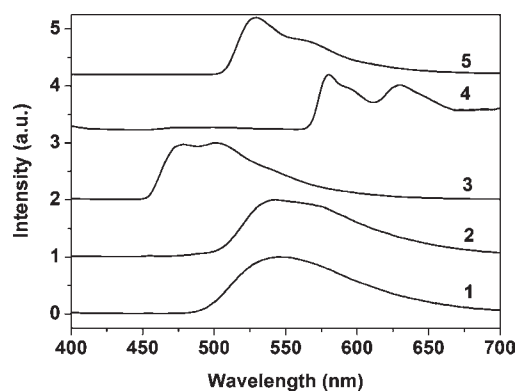
Figure 4. Normalized emission spectra of **1**−**5** in EtOH glass at 77 K.
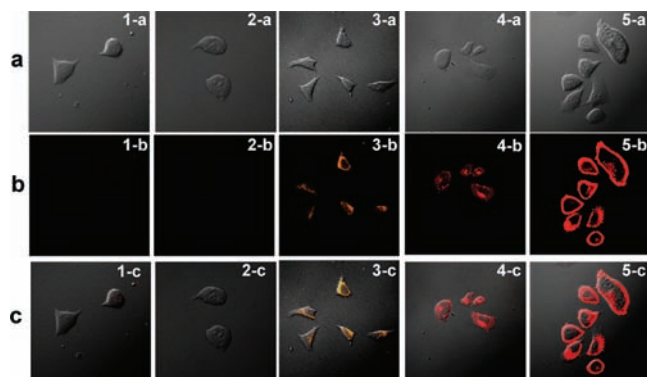
Figure 5. Brightfield images (a), confocal luminescence imaging (b), and overlays (c) of living KB cells incubated with complexes **1**−**5** (20 μM) for 30 min.

the same reason, their amphiphilicity changes from hydrophilic to hydrophobic with log $P_{o/w}$ changing from −1.89 (complex **1**) to 1.39 (complex **5**). The liposomes, composed of double phospholipid layers similar to cell membranes, can encapsulate both hydrophilic and hydrophobic compounds.[67,68] The encapsulation efficiency of the complexes into liposomes, and their release from the liposomes reflects the characteristic of the complexes' permeation in and release outside of the bilayer of the cell membrane, respectively.[69] After long-period equilibrium, the encapsulation efficiency for the compounds are obviously different. Complexes **1** and **2** were encapsulated by nearly 50%, while compound **5** reached 83%. Data fairly show the encapsulation efficiency of these

(67) Le, U. A.; Cui, Z. R. *Int. J. Pharm.* **2006**, *312*, 105–112.
(68) Abraham, S. A.; Edwards, K.; Karlsson, G.; MacIntosh, S.; Mayer, L. D.; McKenzie, C.; Bally, M. B. *Biochim. Biophys. Acta* **2002**, *1565*, 41–54.
(69) Ghezzi, A.; Aceto, M.; Cassino, C.; Gabano, E.; Osella, D. *J. Inorg. Biochem.* **2004**, *98*, 73–78.
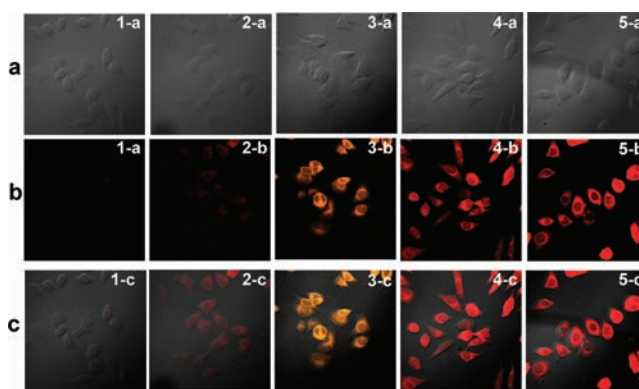
Figure 6. Brightfield images (a), confocal luminescence imaging (b), and overlays (c) of fixed KB cells incubated with complexes **1**−**5** (10 μM) for 30 min.

Table 7. Solubility, log $P_{o/w}$, Encapsulation Efficiency, and Release for Complexes **1**−**5**

complex	solubility (μM)	log $P_{o/w}$	encapsulation efficiency (%)	release (%)
1	2064	−1.89	49.9	39.6
2	5096	−0.88	56.1	33.5
3	559	−0.55	59.2	29.1
4	174	0.69	77.9	20.7
5	37	1.39	83.1	17.4
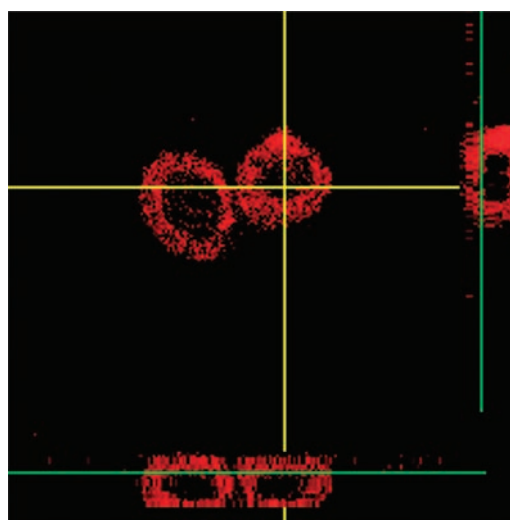
Figure 7. Z-scan images of living KB cells incubated with complex **5**.

iridium(III) complexes follows the order **1** < **2** < **3** < **4** < **5**, which is in keeping with the same trend with lipophilicity and is inverse to the release order. The release for complex **5** is 17.4%, less than half of that for complex **1**. Subsequently, the hydrophilic molecules are difficult to

be encapsulated and easy to release from the cell membrane, whereas the hydrophobic ones are more likely to stay inside the cell. That is, the cellular uptake efficiencies of materials increase with enhancement of their lipophilicity; thus, amphiphilic complexes are the best choice in view of the hydrophilic environment around cells and the amphiphilic character of cell membranes. These rules indicate that in molecular designing for cell imaging, the key point is the amphiphilicity of the molecules, but not the larger the hydrophicity is the better the imaging effect will be.

Conclusions

We synthesized a series of zwitterionic iridium(III) complexes, $Ir(C^{\wedge}N)_2(Hdcbpy)$, whose structures were confirmed by X-ray crystal data. All of these compounds could be dissolved in PBS (pH 7.0) with different solubilities because of the introduction of hydrophilic carboxyl groups on the Hdcbpy ligand. Theoretical calculations show that for these complexes, the nature of the excited states contains ^3MLCT, ^3LLCT, ^3LC as well as ^3ILCT. Photophysical properties in PBS, CH_2Cl_2, and EtOH were studied, and intensive emissions with high quantum yields were observed. As their

lipophilic part (cyclometalating ligands) gradually changed, the amphiphilicity of the complexes also changed. The compounds were finally used in aqueous solution as luminescent dyes for imaging both living and fixed KB cells. An obvious difference in the cell permeation for the complexes was found, which was further proved by the encapsulation and release experiments. The investigation on the lipophilicity, the encapsulation, and release of these complexes shows that the key point in the molecular designing for cell imaging is the amphiphilicity of the molecules: the hydrophilic part is needed for the solubility in aqueous solution while the lipophilic part is helpful for the cell permeation.

Supporting Information Available: X-ray crystallographic data of complexes **1** and **2** in CIF format, optimized data of **1** and **2**, and Z-scan images of living KB cells incubated with complex **5**. This material is available free of charge via the Internet at http://pubs.acs.org.